

# Endogenous lectins from cultured cells: Nuclear localization of carbohydrate-binding protein 35 in proliferating 3T3 fibroblasts

(cell growth/density-dependent growth control/immunofluorescence/immunoblotting)

IOANNIS K. MOUTSATSOS\*, MARGARET WADE†, MELVIN SCHINDLER\*, AND JOHN L. WANG\*

\*Department of Biochemistry, Michigan State University, East Lansing, MI 48824; and †Meridian Instruments, Inc., 2310 Science Parkway, Okemos, MI 48864

Communicated by N. Edward Tolbert, June 8, 1987

**ABSTRACT** Proliferating 3T3 mouse fibroblasts contain higher levels of the lectin carbohydrate-binding protein 35 (CBP35) than do quiescent cultures of the same cells. An immunofluorescence study was carried out with a rabbit antiserum directed against CBP35 to map the cellular fluorescence distribution in a large population of cells under different growth conditions. This cytometric analysis showed that the lectin is predominantly localized in the nucleus of the proliferating cells. In quiescent 3T3 cultures, the majority of the cells lost their nuclear staining and underwent a general decrease in the overall fluorescence intensity. Stimulation of serum-starved quiescent 3T3 cells by the addition of serum resulted in an increase in the level of CBP35. The percentage of cells showing distinct punctate intranuclear staining reached a maximum at about the same time as the onset of the first S-phase of the cell cycle. All of these results suggest that CBP35 may be a protein whose presence in the nucleus, in discrete punctate distribution, is coordinated with the proliferation state of the cell.

In previous studies, we reported the isolation, from 3T3 mouse fibroblasts, of three carbohydrate-binding proteins (CBPs), all of which bind galactose-containing glycoconjugates (1, 2). These were designated CBP35 ( $M_r$  35,000), CBP16 ( $M_r$  16,000), and CBP13.5 ( $M_r$  13,500). A polyclonal rabbit antiserum specific for CBP35 was used to analyze the subcellular localization (3) and tissue distribution (4) of the lectin. These studies revealed that the majority of CBP35 was associated with the cytoplasmic fraction and the nucleus of the 3T3 cell. In addition, CBP35 was identified in adult and embryonic mouse tissues that contained proliferating cell populations (e.g., embryonic liver and skin). In contrast, the lectin was not detected in several adult tissues whose predominant cell population was quiescent (e.g., adult liver and brain).

The association of CBP35 with the nucleus and the apparent correlation with proliferating cell populations prompted us to analyze the level of this protein in 3T3 mouse fibroblasts under proliferating and quiescent conditions. In the present communication, we introduce the technique of automated single-cell analysis of fluorescence in anchored cells in tissue culture to document proliferation-dependent expression and nuclear localization of CBP35. This expression of CBP35 and its nuclear translocation are apparently regulated during the  $G_1$  phase of the cell cycle.

## MATERIALS AND METHODS

**Cell Culture and Synchronization.** Swiss 3T3 fibroblasts were cultured in Dulbecco's modified Eagle's medium (KC Biological, Lenexa, KS) containing 10% calf serum (Microbiological Associates, Walkersville, MD). Cells cultured at a

density less than  $5 \times 10^4$  cells per  $\text{cm}^2$  were proliferative and incorporated [ $^3\text{H}$ ]thymidine; above this density, the cells remained in a quiescent monolayer state (5). Cells at low density were arrested by removal of serum and maintenance in medium containing 0.2% calf serum for 48 hr. Upon readdition of serum (10%), the cells were stimulated to proceed into the cell cycle in a synchronous fashion.

DNA synthesis was assayed by the incorporation of [ $^3\text{H}$ ]thymidine (1.9 Ci/mmol, Schwarz/Mann; 1 Ci = 37 GBq). Cultures were pulse-labeled with radioactive thymidine (2  $\mu\text{Ci}$  per culture) for 1 hr, washed with phosphate-buffered saline (10 mM sodium phosphate/0.14 M NaCl/4 mM KCl, pH 7.4), and detached from the growth surface with trypsin (6). After centrifugation and resuspension in phosphate-buffered saline, the number of cells was determined; aliquots of the cell suspension corresponding to  $5 \times 10^5$  cells were centrifuged in a Beckman Microfuge for 8 sec, and the pelleted cells were solubilized in 0.1 M NaOH/1% (wt/vol) NaDodSO<sub>4</sub> and subjected to scintillation counting (6).

**Immunoblotting and Quantitation of CBP35.** Cells were removed from the culture dish with trypsin, washed, and centrifuged. After resuspension in phosphate-buffered saline,  $5 \times 10^5$  cells were centrifuged in a Beckman Microfuge for 8 sec, solubilized in 40  $\mu\text{l}$  of NaDodSO<sub>4</sub>/PAGE sample buffer, and heated to 90°C for 15 min. The samples were then analyzed in NaDodSO<sub>4</sub>/PAGE (3, 7). Subcellular fractionation was carried out as previously described (3). Material corresponding to the cytoplasmic (S150) and nuclear (pellet) fractions derived from both density-inhibited and serum-stimulated cells was analyzed.

After electrophoresis, the separated proteins were transferred to nitrocellulose filters and immunoblotted with a rabbit antiserum directed against CBP35. The generation and characterization of the specificity of this antiserum have been reported (2-4). The binding of rabbit anti-CBP35 to the  $M_r$  35,000 polypeptide on the nitrocellulose paper was revealed with the colored product of the horseradish peroxidase (HRP) reaction derived from HRP-conjugated goat antibodies directed against rabbit immunoglobulin (Bio-Rad).

Two alternative methods were used to quantitate the amount of CBP35 in the samples. In the first method, the nitrocellulose filters containing the HRP-reactive bands were photographed on Kodak precision-line LPD4 film (Eastman Kodak), and the intensity of the immunoreactive bands was quantitated by densitometric scanning of the film. In the second method, the stained bands corresponding to CBP35 were excised and incubated in 75 mM Tris-HCl/0.5 M NaCl, pH 7.5, containing bovine serum albumin (1%, wt/vol) for 10 min. The nitrocellulose strips were then incubated in the same buffer containing  $2.5 \times 10^5$  cpm/ml of  $^{125}\text{I}$ -labeled (8) protein A (Miles) for 1 hr at room temperature. The nitrocellulose strips were washed three times (10 min each) and

The publication costs of this article were defrayed in part by page charge payment. This article must therefore be hereby marked "advertisement" in accordance with 18 U.S.C. §1734 solely to indicate this fact.

Abbreviations: CBP, carbohydrate-binding protein; HRP, horseradish peroxidase.

assayed for  $\gamma$  radioactivity. Bands on the same immunoblot were compared directly. Both assays were linear over the range of protein concentrations used.

**Immunofluorescence and Digital Image Analysis.** Culture and labeling of 3T3 cells with rabbit anti-CBP35 and rhodamine- or fluorescein-conjugated goat anti-rabbit immunoglobulin (Miles) have been described (3). To obtain a quantitative assessment of antibody labeling in a large number of cells, we used the ACAS 470 Fluorescence Workstation (Meridian Instruments, Okemos, MI), an automated, laser-based digital imaging system designed to perform quantitative and distributional analysis of fluorescence intensity of anchorage-dependent single cells in tissue culture.

The standard instrument was equipped with a 2W argon-ion laser (for rhodamine, dichroic and barrier filters at 580 nm; for fluorescein, dichroic and barrier filters at 510 and 515 nm, respectively), inverted phase-contrast microscope, microstepping stage, and 16-bit microcomputer for data acquisition. As the stage moves in an  $x$ - $y$  raster pattern, the attenuated laser beam, focused to  $\approx 1 \mu\text{m}$ , excites the fluorescence in cells at 1.5- $\mu\text{m}$  step intervals. The emission is recorded by the photomultiplier tube and digitized by the computer. Information is displayed on the video screen as a 16-color image of the fluorescent distribution. Several fields of view were analyzed with the same instrument settings and the  $\times 40$  phase objective (total magnification =  $\times 400$ ). The data were plotted in histogram form.

## RESULTS

**Analysis of the Immunofluorescence Patterns for CBP35 at Different Cell Densities.** In previous immunofluorescence studies, we had observed intracellular staining of mouse 3T3 fibroblasts by rabbit anti-CBP35 antiserum (3). This antiserum (*i*) immunoblots a single polypeptide ( $M_r$  35,000) in NaDodSO<sub>4</sub> extracts (3) and in Triton X-100 extracts (4) of 3T3 cells, (*ii*) isolates CBP35 from Triton X-100 extracts of 3T3 cells by immunoaffinity chromatography (3), and (*iii*) immunoprecipitates CBP35 out of a partially purified preparation of endogenous lectins derived from 3T3 cells (2). Therefore, rabbit anti-CBP35 was monospecific in its recognition of CBP35 in both denatured and nondenatured protein mixtures. With this antiserum, the staining was localized mainly in the nucleus of some cells; in other cells, the staining was diffusely distributed in the cytoplasm. This disparity in the staining patterns did not appear to be due to immunodetection of antigens other than CBP35 because similar results also were obtained with rabbit anti-CBP35 antibodies affinity-purified by the procedure of Smith and Fisher (9). Rather, the labeling patterns were apparently dependent on the density of the culture on which the immunofluorescence was performed.

Cultures of 3T3 cells were seeded at different densities; after an overnight period of attachment, the cultures were subjected to immunofluorescence analysis with rabbit anti-CBP35. Representative epifluorescence photographs for three different cell densities are shown in Fig. 1. Qualitatively, these photographs indicate the following: (*i*) in sparse cultures ( $3 \times 10^3$  cells per  $\text{cm}^2$ ), there was intense staining of the cells, predominantly in the nucleus; (*ii*) in subconfluent cultures ( $2 \times 10^4$  cells per  $\text{cm}^2$ ), the staining intensity decreased and the nuclear localization was less distinct; and (*iii*) in confluent monolayers ( $5 \times 10^4$  cells per  $\text{cm}^2$ ), there was faint staining of the cytoplasm, with little or no staining of the nucleus. Consistent with previous experiments (3), control samples stained with preimmune rabbit serum showed no fluorescent labeling under all three culture conditions.

Using the ACAS 470 Fluorescence Workstation, we examined the distribution of CBP35 in labeled cells by fluorescence digital imaging, taking advantage of the instrument's

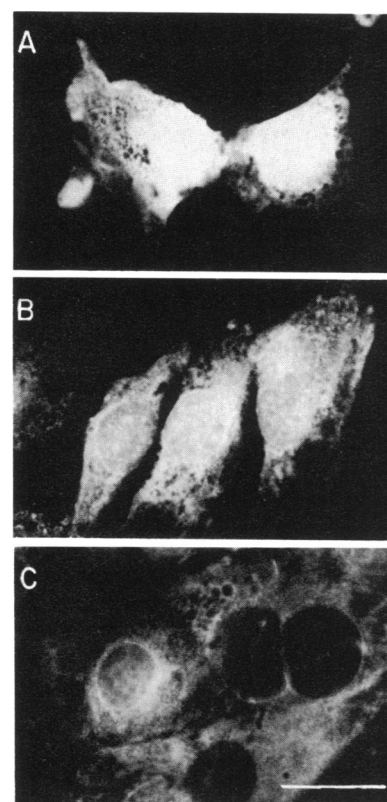


FIG. 1. Immunofluorescence staining for CBP35 in 3T3 fibroblasts after fixation with formaldehyde (3.7%) and permeabilization with Triton X-100 (0.2%). The binding of rabbit anti-CBP35 (1:5 dilution of antiserum; 2 hr at room temperature) was detected by rhodamine-labeled goat anti-rabbit immunoglobulin (1:30 dilution; 0.5 hr at room temperature). Cell densities were used:  $3 \times 10^3$  cells per  $\text{cm}^2$  (sparse) (A),  $2 \times 10^4$  cells per  $\text{cm}^2$  (subconfluent) (B), and  $5 \times 10^4$  cells per  $\text{cm}^2$  (confluent) (C). (Bar = 50  $\mu\text{m}$ .)

analytical capabilities to display a population analysis of CBP35 concentration per cell in a large number of cells ( $\approx 60$  cells per analysis). Fig. 2 shows a series of pseudocolor fluorescence intensity maps of the distribution of CBP35 in cells from sparse (column A), subconfluent (column B), and confluent (column C) cultures. A number of such image fields were recorded, and a histogram was generated representing the total number of cells with a particular integrated fluorescence intensity (Fig. 2). This quantitative analysis on single cells yielded conclusions that are consistent with the qualitative observations made on the epifluorescence photographs (Fig. 1). First,  $>50\%$  of the cells in sparse cultures (Fig. 2A) were intensely labeled (defined as  $>6$  on the intensity scale of the histograms); a few cells had little or no labeling for CBP35. In labeled cells, the intensity was highest at the cell nucleus, with little staining in the cytoplasm. Second, cells at subconfluence (Fig. 2B) showed a decrease in overall fluorescence intensity. Only 18% of the cells were intensely labeled. Finally, cells in a confluent monolayer (Fig. 2C) showed no nuclear staining and demonstrated an overall fluorescence intensity that was slightly above background. Less than 8% of the cells were intensely labeled. All of these results indicate that the amount of detectable CBP35, as well as its subcellular distribution, are dependent on the condition of the cell culture under analysis.

**Quantitation of CBP35 in Proliferating and Quiescent 3T3 Cells.** To determine the amount of CBP35 in proliferating and quiescent 3T3 cells, two different protocols were used: (*i*) density-arrested confluent monolayers of 3T3 cells were stimulated to undergo one round of DNA synthesis and cell division by the addition of serum; and (*ii*) sparse cultures of

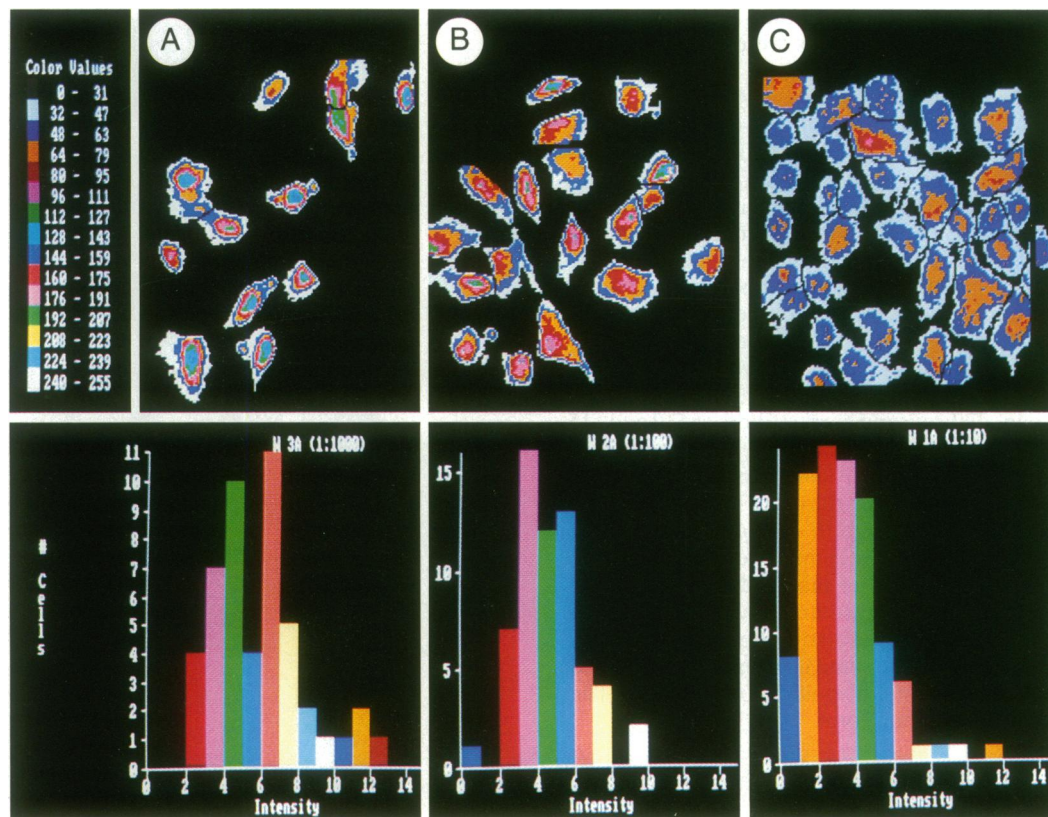


FIG. 2. Analysis of the rabbit anti-CBP35 immunofluorescence patterns on 3T3 cells using the ACAS 470 Fluorescence Workstation. The cells were labeled as described in the legend to Fig. 1. Cell densities were:  $3 \times 10^3$  cells per  $\text{cm}^2$  (sparse) (A),  $2 \times 10^4$  cells per  $\text{cm}^2$  (subconfluent) (B), and  $5 \times 10^4$  cells per  $\text{cm}^2$  (confluent) (C). (Upper) Pseudo color fluorescence intensity maps (the scale on the left provides the fluorescence intensity color code). Errors in measurements could result in a shift of one color unit in the fluorescence intensity color code. (Lower) Histograms representing the number of cells recording a particular integrated fluorescence intensity. All histograms were scaled to a maximum intensity value of 50,000 arbitrary fluorescence units.

3T3 cells were deprived of serum to induce quiescence and restimulated by the addition of serum. Confluent monolayers of 3T3 cells exhibit density-dependent inhibition of growth (5); a low level of DNA synthesis was observed (Fig. 3A). Upon addition of serum, the level of [ $^3\text{H}$ ]thymidine increased approximately 6-fold 20 hr later. Over the same period, serum addition also increased the amount of CBP35 by about 3.5-fold (Fig. 3B). Using the subcellular fractionation procedure described previously (3), we also have isolated the cytoplasmic (S150) and nuclear (pellet) fractions derived from density-inhibited 3T3 cells and from parallel monolayers that were serum-stimulated. The level of CBP35 was 2.6-fold higher in the nuclei derived from serum-stimulated 3T3 monolayers than in the nuclei derived from quiescent monolayers (Fig. 4B); little difference in the level of CBP35 was found in the cytoplasmic fractions (Fig. 4A). These results indicate that the amount of CBP35 in the nucleus may correlate with the proliferative state of the cell.

Similar results were also obtained with sparse cultures of 3T3 cells. After serum starvation to arrest the cells, addition of serum increased DNA synthesis as well as the amount of CBP35. Thus, it appears that the correlation between CBP35 expression and proliferation is independent of cell density and of the method by which quiescence was achieved.

**Immunofluorescence of CBP35 in Synchronized 3T3 Cells.** When serum-starved, sparse cultures of 3T3 cells were stimulated by the addition of serum, the first wave of DNA synthesis in the synchronized cells was observed between 16 and 28 hr after serum addition (Fig. 5A). Samples from parallel cultures were subjected to immunofluorescence staining with rabbit anti-CBP35. These immunofluorescence slides were analyzed by the ACAS 470 Fluorescence Work-

station, and histograms representing the number of cells recording a particular integrated fluorescence intensity were generated in the same manner as the experiments shown in

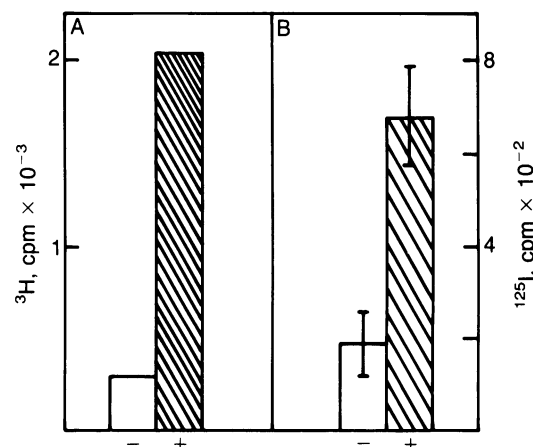


FIG. 3. Comparison of the increase in level of DNA synthesis (A) and level of CBP35 (B) when density-inhibited 3T3 monolayers ( $5 \times 10^4$  cells per  $\text{cm}^2$ ) were stimulated by the addition of calf serum (10%). DNA synthesis was assayed by the incorporation of [ $^3\text{H}$ ]thymidine ( $2 \mu\text{Ci}$  per culture for 1 hr at  $37^\circ\text{C}$ ) (A). CBP35 was quantitated by NaDodSO<sub>4</sub>/PAGE of extracts of cultures followed by immunoblotting analysis using rabbit anti-CBP35, HRP-conjugated goat anti-rabbit immunoglobulin, and  $^{125}\text{I}$ -labeled protein A as described (B). The data for CBP35 quantitation represent the average of triplicate determinations ( $\pm$  SEM). The assays were carried out 20 hr after the addition of calf serum (hatched bars). Control cultures that received no calf serum (open bars) were analyzed in parallel.

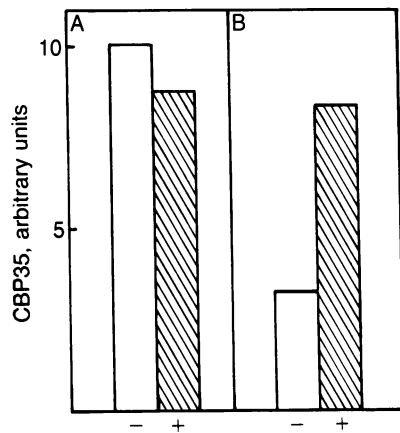


FIG. 4. Comparison of the increase in the level of CBP35 in the cytoplasmic (S150) fraction (A) and the nuclear pellet (B) when density-inhibited 3T3 monolayers ( $5 \times 10^4$  cells per  $\text{cm}^2$ ) were stimulated by the addition of calf serum (10%). Subcellular fractionation was carried out as described (3), and the corresponding fractions (40  $\mu\text{g}$  of protein) were compared by NaDodSO<sub>4</sub>/PAGE and immunoblotting analysis. CBP35 was quantitated by densitometric scanning of the film containing the HRP-stained bands. The assays were carried out 20 hr after the addition of calf serum (hatched bars). Control cultures that received no calf serum (open bars) were analyzed in parallel.

Fig. 2. All cells with an integrated fluorescence intensity of  $>4$  were defined as labeled cells. This analysis showed that the percentage of labeled cells increased with time after serum addition (Fig. 5B). The increase in CBP35 occurred well before the onset of S phase in the synchronized cell population.

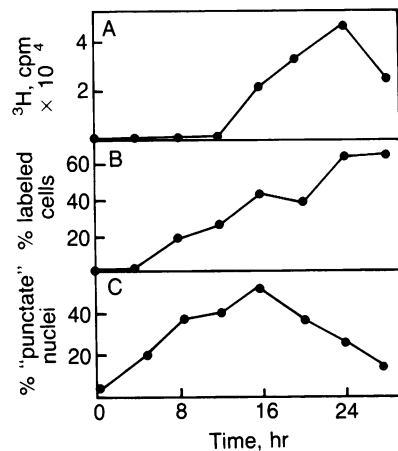


FIG. 5. Comparison of the changes in the level of DNA synthesis (A), the percentage of cells stained with rabbit anti-CBP35 antiserum (B), and the percentage of fluorescent nuclei that showed punctate intranuclear staining (C) in synchronized 3T3 cell populations during the cell cycle. 3T3 cells ( $10^4$  cells per  $\text{cm}^2$ ) were synchronized by serum starvation (48 hr at 0.2% calf serum). Cells were restimulated by the addition of calf serum (10%); at various times thereafter, samples containing  $5 \times 10^5$  cells were analyzed for DNA synthesis by the incorporation of [<sup>3</sup>H]thymidine (2  $\mu\text{Ci}$  per culture for 1 hr at 37°C). At the same time points, cells were fixed and processed for immunofluorescence staining by rabbit anti-CBP35 and fluorescein-labeled goat anti-rabbit immunoglobulin. The cultures were then analyzed by using the ACAS 470 Fluorescence Workstation. Scans of cultures and their corresponding fluorescence intensity histograms were constructed. In B, the percentage of cells registering a fluorescence intensity of 4 or above (on an arbitrary scale of 1–12) were considered as staining positively for CBP35. In C, the number of cells with nuclear staining were scored, and the percentage of labeled nuclei exhibiting punctate intranuclear staining is shown.

The pattern of intracellular staining in serum-starved, quiescent 3T3 cells and in serum-stimulated, proliferating cells was similar to those obtained for cells in confluent and sparse cultures (Fig. 1). Serum-starved, quiescent cells showed little fluorescence staining with rabbit anti-CBP35 (Fig. 5B). Of the stained cells,  $\approx 50\%$  showed staining of the nucleus. In Fig. 6A, a nucleus with a granular staining pattern is shown alongside a diffusely and weakly labeled nucleus (indicated by arrow). Sixteen hours after serum stimulation, 85% of the fluorescent cells showed nuclear staining. Punctate intranuclear (possibly nucleolar) staining was prominent in  $\approx 50\%$  of the labeled nuclei (Fig. 6B). Twenty hours after serum addition, 68% of the fluorescent cells had stained nuclei. Characteristic patterns include diffuse nuclear staining (62% of nuclear positive cells) and punctate staining (38% of nuclear positive cells) (Fig. 6C).

When the percentage of stained nuclei showing punctate intranuclear staining was plotted as a function of time after serum stimulation, there was a distinct maximum at about 16 hr (Fig. 5C). A similar profile was observed when the percentage of nuclear positive cells was plotted as a function of time after the addition of serum. Thus, it appears that although the overall percentage of CBP35-positive cells increased monotonically with serum stimulation, the nuclear

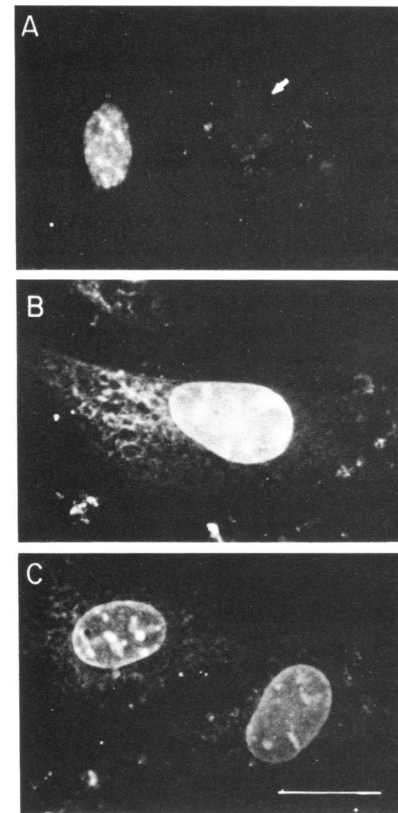


FIG. 6. Fluorescence staining patterns of rabbit anti-CBP35 antiserum in serum-starved 3T3 cells at various times after serum stimulation. Cells were synchronized and stained for immunofluorescence as described in the legend to Fig. 5. (A) Serum-starved quiescent 3T3 cells showing a nucleus with a granular staining pattern and a weak, diffusely stained nucleus (white arrow). Most of the cells were not fluorescent; of the fluorescent cells,  $\approx 50\%$  showed nuclear staining. (B) Serum-starved 3T3 cells treated with serum for 16 hr showed prominent punctate intranuclear staining. Approximately 85% of fluorescent cells showed nuclear staining; of this, 53% showed a punctate labeling pattern. (C) Serum-starved 3T3 cells treated with serum for 20 hr showed diffuse nuclear staining as well as punctate intranuclear staining. Approximately 62% of the fluorescent cells showed diffuse nuclear staining while 38% had distinct punctate labeling. (Bar = 50  $\mu\text{m}$ .)

localization showed a rise and a fall. The maximum in this kinetic profile was at  $\approx 16$  hr after serum addition, corresponding to the beginning of the S phase of the synchronized cell population (Fig. 5A).

**Comparison of the Expression of CBP35 in Normal and Transformed 3T3 Cells.** The amount of CBP35 in normal 3T3 fibroblasts was compared to that in 3T3 cells transformed by Kirsten murine sarcoma virus. In confluent monolayers, normal 3T3 cells are subject to density-dependent inhibition of growth; these quiescent cells contain little CBP35. By contrast, the virally transformed cells continue to proliferate at high density, and these cells have  $\approx 18$  times more CBP35 than their normal counterparts. Similar results were also obtained when the amounts of CBP35 in these two cell types were compared under sparse culture conditions.

## DISCUSSION

The data documented in the present communication indicate: (i) proliferating 3T3 cells have a higher level of the lectin CBP35 than do quiescent cultures of the same cells; (ii) in proliferating cells, the lectin is primarily in the nucleus, whereas the protein is mostly cytoplasmic in quiescent 3T3 cells; (iii) immunofluorescence analysis of CBP35 within the nucleus shows a punctate staining pattern, possibly reflecting an association of the lectin with nucleolar structures; and (iv) upon addition of serum to serum-starved, quiescent 3T3 fibroblasts, the percentage of cells immunofluorescently stained with anti-CBP35 antiserum increased during the early part of the G<sub>1</sub> period. This increase continued as the population of synchronized cells entered into S phase. In contrast to the monotonic overall increase in CBP35-positive cells upon serum stimulation, there was a distinct rise and fall in the localization of CBP35 in the nucleus during the same time course. This may indicate that the nuclear localization of CBP35 is cell cycle dependent.

These results need to be considered in the context of the recent reports on sugar-binding sites in mammalian cell nuclei (10, 11). Using quantitative flow microfluorometry of neoglycoprotein binding, Sève and co-workers have demonstrated the existence of sugar-binding sites (lectin-like molecules) in isolated baby hamster kidney (BHK) cell nuclei. Fluorescence microscopy further indicated that in the nuclear preparations, the neoglycoprotein binding sites may be associated with the nucleoli as well as with nucleoplasmic ribonucleoprotein elements. Moreover, nuclei from exponentially growing cells bound much more of the neoglycoprotein than did nuclei from contact-inhibited cells.

In the light of these observations, it is intriguing to consider the possibility that the nuclear sugar-binding sites might include CBP35. The saccharide-binding specificity of CBP35 (2, 4) would be consistent with the observed binding of lactose-derivatized bovine serum albumin (11). It should also be noted that Feizi and co-workers have localized a bovine heart lectin ( $M_r$  13,000, possibly corresponding to CBP13.5) at the nucleus of cells, using a polyclonal antibody on cryostat sections of tissues (12) and a monoclonal antibody on lymphoid cells (13). The level and pattern of expression of their lectin in lymphoid cells changed in association with transformation or after stimulation with mitogens. Finally, observations consistent with the nuclear localization of  $\beta$ -galactoside-binding lectins in epithelial tissues have also been reported by Beyer and Barondes (14).

The physiological function of CBP35 is not known. The fact that proliferating cells show higher levels of CBP35 and other sugar-binding sites in the nucleus suggests that this group of lectin-related proteins may be components of growth regulatory systems that are elicited in stimulated and transformed cells. In any case, all of these recent observations on the localization of lectins in the nucleus provoke the search for a nuclear component with which CBP35 interacts.

Besides these considerations on the function of CBP35, the results of our present study also provide a basis for understanding several observations made in previous studies. We had noted that an apparently higher level of CBP35 was detected in the nucleus of 3T3 fibroblasts by indirect immunofluorescence than by immunoblotting analysis of subcellular fractions (3). This is due, at least in part, to the fact that we had used high-density cultures to maximize the number of cells as starting material for subcellular fractionation on sucrose gradients. In addition, the present results are also consistent with previously reported immunoblotting analyses of CBP35 in various cell lines and tissues of the mouse (4). There was more CBP35 in Kirsten murine sarcoma virus-transformed 3T3 cells than in untransformed 3T3 fibroblasts. Similarly, there was more CBP35 detectable in Rous sarcoma virus-transformed chicken embryo fibroblasts than in the normal counterparts. Raz *et al.* (15) have identified two lectins ( $M_r$  34,000 and  $M_r$  68,000) that are present in high amounts in tumor cells and have termed them tumor cell lectins. This may reflect increased levels of expression of the normal cell gene product in the transformed cells. They have also found that most of the lectin(s) is inside the B16-F1 melanoma cell, as is the case for CBP35 in 3T3 fibroblasts (3).

This work was supported by Grants GM-27203 (to J.L.W.), GM-32310 (to J.L.W.), and GM-30158 (to M.S.) from the National Institutes of Health and SBIR IR 43 CA-39945 (to Meridian Instruments). J.L.W. was supported by Faculty Research Award FRA-221 from the American Cancer Society.

1. Roff, C. F., Rosevear, P. R., Wang, J. L. & Barker, R. (1983) *Biochem. J.* **211**, 625–629.
2. Roff, C. F. & Wang, J. L. (1983) *J. Biol. Chem.* **258**, 10657–10663.
3. Moutsatsos, I. K., Davis, J. M. & Wang, J. L. (1986) *J. Cell Biol.* **102**, 477–483.
4. Crittenden, S. L., Roff, C. F. & Wang, J. L. (1984) *Mol. Cell Biol.* **4**, 1252–1259.
5. Todaro, G. J. & Green, H. (1963) *J. Cell Biol.* **17**, 299–313.
6. Steck, P. A., Voss, P. G. & Wang, J. L. (1979) *J. Cell Biol.* **83**, 562–575.
7. Laemmli, U. K. (1970) *Nature (London)* **227**, 680–685.
8. Fraker, P. J. & Speck, J. C. (1978) *Biochem. Biophys. Res. Commun.* **80**, 849–857.
9. Smith, D. E. & Fisher, P. A. (1984) *J. Cell Biol.* **99**, 20–28.
10. Sève, A. P., Hubert, J., Bouvier, D., Bouteille, M., Maintier, C. & Monsigny, M. (1985) *Exp. Cell Res.* **157**, 533–538.
11. Sève, A. P., Hubert, J., Bouvier, D., Bourgeois, C., Midoux, P., Roche, A. C. & Monsigny, M. (1986) *Proc. Natl. Acad. Sci. USA* **83**, 5997–6001.
12. Childs, R. A. & Feizi, T. (1980) *Cell Biol. Int. Rep.* **4**, 755.
13. Carding, S. R., Thorpe, S. J., Thorpe, R. & Feizi, T. (1985) *Biochem. Biophys. Res. Commun.* **127**, 680–686.
14. Beyer, E. C. & Barondes, S. H. (1980) *J. Supramol. Struct.* **13**, 219–227.
15. Raz, A., Meromsky, L., Carmi, P., Karakash, R., Lotan, D. & Lotan, R. (1984) *EMBO J.* **3**, 2979–2983.